Hearing Research 332 (2016) 46–54

Contents lists available at ScienceDirect

Hearing Research

journal homepage: www.elsevier.com/locate/heares

Research paper

Quantitative PCR analysis and protein distribution of drug transporter genes in the rat cochlea

Senthilvelan Manohar [a], Samson Jamesdaniel [a], Dalian Ding [a], Richard Salvi [a], Gail M. Seigel [a, c], Jerome A. Roth [b, *]

[a] Center for Hearing & Deafness, University at Buffalo, NY 14214, United States
[b] Department of Pharmacology and Toxicology, University at Buffalo, NY 14214, United States
[c] SUNY Eye Institute, New York, United States

ARTICLE INFO

Article history:
Received 12 August 2015
Received in revised form
6 October 2015
Accepted 30 October 2015
Available online 26 November 2015

Keywords:
Membrane transporter
PCR array
Cochlea
Immunohistochemistry

ABSTRACT

Membrane transporters can be major determinants in the targeting and effectiveness of pharmaceutical agents. A large number of biologically important membrane transporters have been identified and localized to a variety of tissues, organs and cell types. However, little is known about the expression of key membrane transporters in the inner ear, a promising site for targeted therapeutics, as well as a region vulnerable to adverse drug reactions and environmental factors. In this study, we examined the levels of endogenous membrane transporters in rat cochlea by targeted PCR array analysis of 84 transporter genes, followed by validation and localization in tissues by immunohistochemistry. Our studies indicate that several members of the SLC, VDAC and ABC membrane transporter families show high levels of expression, both at the RNA and protein levels in the rat cochlea. Identification and characterization of these membrane transporters in the inner ear have clinical implications for both therapeutic and cytotoxic mechanisms that may aid in the preservation of auditory function.

1. Introduction

The therapeutic effectiveness of many drugs and biologically active agents is critically dependent on their access to and uptake into specific tissues within the body. The cellular uptake of most drugs is a highly selective process carried out in large part by a diverse array of membrane-bound transporters which generate cellular levels that are therapeutically effective or in some cases toxic. It has been estimated there are over 1500 human transporter genes which encode transporters or transport-related proteins that regulate the cellular uptake, sequestration and efflux of numerous physiological active endogenous and foreign compounds (Drake et al., 2014). Defective transporters can provoke a variety of pathological conditions (Camacho et al., 2003; Kobayashi et al., 2012; Seow et al., 2004) because of their deleterious influence on cellular levels of endogenous substrates as well as by altering the uptake and elimination of drugs (Letschert et al., 2004; Roth et al., 2012; Thompson et al., 2011; Torres et al., 2011). The functional performance of these transporters is genetically controlled and genetic polymorphisms can result in reduced expression or altered performance (De Mattia et al., 2013; Drake et al., 2014; Ishikawa et al., 2005). The extent to which these transport proteins contribute to the accumulation of drugs and other foreign agents is often influenced indirectly by a variety of aberrant biochemical and molecular processes which adapt to cellular demands placed on it by the nutritional requirements of endogenous substances. The expression of these transporters can similarly be modified by drugs, sometimes with deleterious consequences.

The solute carrier (SLC) superfamily of transporters represents one example of essential membrane-bound proteins responsible for trafficking a diverse set of endogenous and exogenous molecules and drugs. The SLC transporters are responsible for the translocation of selective substrates across biological membranes through a variety of biochemical processes that include facilitated diffusion, ion coupling, and ion exchange which participate in the delivery of drugs. In some cases, this process is triggered by an ion gradient that is maintained by active transporters of the ATP-binding cassette (ABC) superfamily of transporters (Greenberg, 2013; Hawley et al., 2013; Wen et al., 2013). Thus, both the SLC and ABC family of transporters represent important proteins

* Corresponding author. Department of Pharmacology and Toxicology, 11 Cary Hall, University at Buffalo, Buffalo, NY 14214, United States.
E-mail address: jaroth@buffalo.edu (J.A. Roth).

http://dx.doi.org/10.1016/j.heares.2015.10.020
0378-5955/

required for the selective delivery, distribution and behavior of many molecules and therapeutic drugs within different organs of the body.

One sensory organ that has received relatively little attention regarding transporters and drug accumulation is the inner ear, even though numerous studies indicate that a variety of therapeutic agents can affect hearing. Surprisingly, the few studies that have assessed the distribution and levels of drug transporters within different portions of the inner ear suggest that uptake is a highly selective process. For example, recent studies in our laboratory have shown that the relative levels and distribution of three divalent cation SLC transporters, SLC11A2 (divalent metal transporter 1), SLC39A8 (ZIP8) and SLC39A14 (ZIP14) vary within the stria vascularis, organ of Corti and spiral ganglion of the cochlea. Individual variations in the levels and/or localization of these and other transporters involved in delivery and export of drugs in the cochlea as well as the presence of functionally inactive mutant forms of these proteins likely account for the degree to which drug-induced hearing impairment is observed. Therefore, it is important to examine the endogenous levels of the different cellular transport systems within the three cellular compartment of the cochlea in order to understand their potential role in regulating pharmacological activity and ototoxicity. To accomplish this, quantitative real-time quantitative PCR (qRT-PCR) studies were performed to analyze the expression of a focused panel of 84 transporter genes in the stria vascularis, basilar membrane and spiral ganglion neurons of the cochlea.

2. Materials and methods

2.1. Animals

Eight male SASCO Sprague-Dawley rats with average weight of 350 g from Charles River Laboratories (Wilmington, MA) were used for this study. The experimental protocol was reviewed and approved by University at Buffalo Institutional Animal Care and Use Committee.

2.2. Total RNA isolation and cDNA construction

The photomicrograph in Fig. 1A *shows a cross section of the cochlea; the colored lines show the approximate boundaries of the stria vascularis (SV, red line) tissue sample, basilar membrane tissue sample (BM, green line) and modiolus (MOD, yellow) tissue sample used for the gene array studies. All samples were consistently and carefully dissected out in an RNAase free environment.* Total RNA was isolated using RNeasy extraction kit (Qiagen) following the manufacturers protocol. Tissue samples were homogenized in RNA free tubes containing QIAzol lysis reagent and centrifuged at 12,000 g at 4 °C for 15 min. The aqueous phases of the samples were transferred to new tubes and an equal volume of 70% ethanol was added and mixed with the samples and transferred to the RNeasy column. The column was incubated with DNase I for 15 min at room temperature to avoid genomic DNA contamination and afterwards total RNA was eluted using 30 μl RNase-free water. Total RNA concentration and purity were measured using a spectrophotometer (Beckman Coulter DU 640 or Thermo Scientific, NanoDrop 2000). Equal concentrations of total RNA (50 ng) were used to construct cDNA using a RT^2 first strand cDNA kit (Cat #: C-03, SA Bioscience Corporation). SuperArray RT qPCR Master Mix (SA Bioscience Corporation) was used for the PCR reaction.

2.3. Gene expression

The drug transporter RT^2 Profiler™ PCR Array (PARN-070Z-SABio-sciences Corp., MD, USA) was used to investigate the expression pattern of genes involved in absorption, distribution, metabolism and excretion of drugs. Since this gene array contains a focused panel of genes related to drug transport, we used this array to investigate the distribution of gene expression in three different cochlear regions. The RT^2 Profiler™ PCR array contained 84 drug transporter genes including genes that regulate the ATP-binding cassette membrane transportation, solute carrier group of membrane transportation, and other types of ionic and voltage gated transportation. In addition, the array has primers for 5 housekeeping genes (ACTB, RPL13A, HPRT1, LDHA, and RPLP1) to facilitate normalization, a genomic DNA primer to detect genomic DNA contamination, 3 reverse transcription controls and 3 positive PCR controls to test the efficiency of cDNA conversion as well as PCR reaction. The PCR reaction was carried out using SYBR Green fluorescence (SABiosciences) technology with 25 μl per reaction in Bio-Rad MyiQ Single Color Real Time PCR System. The PCR program consisted of one cycle of a hot start (95 °C) for 10 min to activate the DNA polymerase and 40 cycles of amplification (95 °C for 15 s, 60 °C for 1 min). Cycle threshold (C_T) values were measured for each gene on the array. *Three repeats of pooled samples were performed for each condition.*

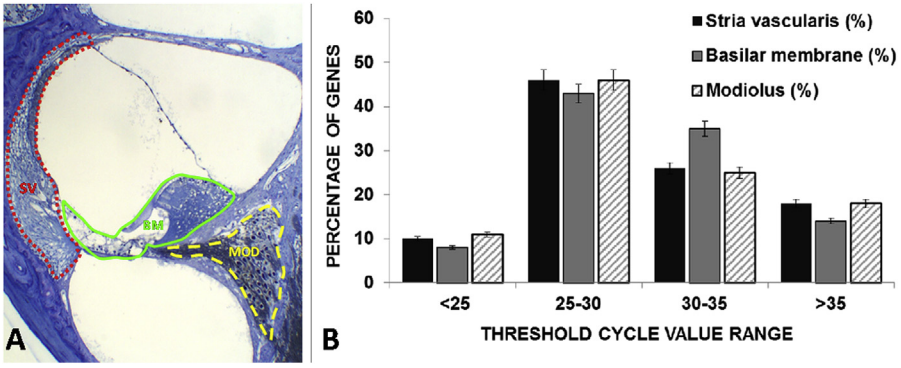

Fig. 1. (A) Photomicrograph of radial section of the cochlea with colored lines demarcating the approximate boundaries of the stria vascularis (SV, red), basilar membrane (BM, green) and modiolus (MOD, yellow) tissue compartments used for qRT-PCR analysis. (B) Percentages of the 84 drug transporter genes with qRT-PCR thresholds cycle (Ct) values in the ranges shown on abscissa. Of the 84 drug transporter genes approximately 85% were classified as detected (Ct $\leq$ 35); ~10% were expressed at high levels (Ct < 25), ~45% at moderate levels (Ct 25–30) and ~28% at low levels (Ct 30–35). (For interpretation of the references to colour in this figure legend, the reader is referred to the web version of this article.)

2.4. Data analysis

The quality of each array PCR reaction run was determined using SA Bioscience online data analysis resource (http://pcrdataanalysis.sabiosciences.com/pcr/arrayanalysis.php). The CT values of five housekeeping genes (Actb, Rpl13a, Hprt1, Ldha, and Rplp1) were averaged and used to normalize the CT values of drug transporter genes to generate ΔCT values. Normalized ΔCT values indicated the relative abundance of each of the 84 drug transporter genes in the stria vascularis, basilar membrane and modiolus.

2.5. Immunochemistry

To identify the distribution and relative expression of specific proteins coded by a subset of specific genes from the PCR array study, immunohistochemical studies were performed using antibodies against Glut1, VDAC 1/2/3, OCT1, OCT2, CD98, and SNAT2. In brief, the cochlear tissue was fixed with 10% formalin in PBS for 4 h at 4 °C. After rinsing with PBS, the cochlear basilar membrane containing the organ of Corti, the spiral ligament containing the stria vascularis and the SGN in Rosenthal's canal were carefully dissected out. Specimens were incubated with 1% Triton X100 and 5% goat serum in 0.1 M PBS plus rabbit primary antibody against Glut1, VDAC 1/2/3, OCT1, OCT2, CD98, or SNAT2 (all from Santa Cruz Biotechnology, Santa Cruz, CA) at a dilution of 1:200 at 4 °C for 24 h. Specimens were then rinsed three times in PBS for 15 min and subsequently incubated for two hours in a solution containing 0.5% TRITC conjugated secondary antibody goat-anti rabbit IgG (Sigma, St. Louis, MO) 5% normal goat serum, 1% Triton X-100 (10%) in 0.01 M PBS. After rinsing with 0.01 M PBS, specimens were stained with Alexa Fluor 488-phalloidin (Invitrogen A12379) to label F-actin expressed on structures in the cochlea, and TO-PRO-3 (Life Technologies) to identify the nucleus. Finally, specimens were mounted on glass slides in glycerin, coverslipped and examined using a confocal microscope (Zeiss LSM-510 Meta) with appropriate filters to detect the green fluorescence of Alexa 488 labeled product to the specific proteins (excitation 488 nm, emission 520 nm). The red fluorescent signal of Alexa 555 in SGN and ANFs was monitored at excitation of 550 nm and emission at 570 nm and purple fluorescence of TO-PRO-3 at excitation of 642 nm and emission at 661 nm. Confocal images were processed using Confocal LSM Image Examiner and Adobe Photoshop 5.5 software as described previously (Ding et al., 2011a). Using the Ortho function feature in the Zeiss LSM Image Examiner software, a single horizontal x–y image plane can be displayed, multiple horizontal images can be merged into a single plane or a z-plane image plane can be reconstructed from a series of horizontal x–y image planes. Immunolabeling with the antibodies used in this study were validated three to five time to confirm that the labeling patterns were consistent across animals.

3. Results

3.1. Gene expression

Fig. 1A *is a cross section of the cochlea with colored lines showing the approximate boundaries of the tissue we refer to as "stria vascularis", "basilar membrane" and "modiolus"; the mRNA harvested from these regions was used for the gene array analyses.* In the current study, the abundance of the different drug transporter genes in all three areas of the cochlea were based on the $2^{-\Delta CT}$ calculated by normalization of the raw CT values relative to expression of the housekeeping genes. For our analysis, genes having a $2^{-\Delta CT}$ value greater than 0.15 (Ct < 25, Fig. 1B) were considered to be highly expressed and those possessing a value from 0.001 to 0.12 (Ct 25–30, Fig. 1B) were considered as being moderately expressed. The data presented in Fig. 1B presents the quantitative PCR analysis for all 84 transporter genes in this array. As indicated, nearly 85% of drug transporter genes were detected in all three cochlear regions; 40–45% were moderately expressed, while approximately 8–11% were highly expressed based on this criteria (Fig. 1).

Based on these criteria, the drug transporter genes considered most abundant, those having $2^{-\Delta CT}$ value equal or greater than 0.15 are presented in Tables 1–3 along with the raw CT values. Of the SLC genes, the most abundantly expressed genes based on the $2^{-\Delta CT}$ value in the stria vascularis include SLC3A2, SLC7A8, SLC38A2, SLC31A1 and SLC2A1 (Table 1), in the basilar membrane, Slc3a2, Slc7a8, Slc38a2 and Slc3a1 (Table 2), and in the modiolus, SLC3A1, SLC22A2, SLC38A2, SLC3A2, SLC7A8, SLC16A1 (Table 3). Expression of genes related with voltage-dependent anion channel transportation, Vdac2, Vdac1, and vacuolar H^+ ATPase (Atp6v0c) were also highly expressed in all three cochlear regions studied. Only in modiolus did the gene related with ATP-binding cassette membrane transporter (ABCD3) show $2^{-\Delta CT}$ mRNA levels greater than 0.15. The raw CT values for these genes ranged from about 23 to 25 in all cochlear regions examined and are consistent with their elevated expression in the three areas of the cochlea.

3.2. Immunohistochemistry

3.2.1. SLC2A1 (Glut1) expression in the cochlear tissue

Immunolabeling studies of the cochlea were performed to examine the relative distribution of the highly expressed drug transporter genes determined by the microarray analysis. Initial studies focused on localization of the glucose transporter, SLC2A1. As shown by Fig. 2A, SLC2A1 was expressed in the cytoplasm of inner and outer hair cells and also in the nuclei of cochlear hair cells and supporting cells. In the cochlear lateral wall, SLC2A1 was expressed only in the nuclei of marginal cells in stria vascularis, but was largely undetectable in the intermediate and basal cells of stria vascularis (Fig. 2B). SLC2A1 was strongly expressed in the cytoplasm and nuclei of spiral ganglion neurons, but was not detected in surrounding supporting cells (Fig. 2C).

3.3. VDAC1/2/3 transporter expression in the cochlear tissue

In our gene array analysis, VDAC1 and 2 were highly expressed in all three cochlear regions. Immunohistochemical analysis using an antibody to detect VDAC1/2/3 proteins demonstrated staining in the cytoplasm and nuclei of cochlear hair cells and Hensen's cells in the organ of Corti (Fig. 3A). In the cochlear lateral wall, VDAC1/2/3 was intensely expressed in the cytoplasm of marginal cells in stria vascularis, but not detectable in the intermediate and basal cells of stria vascularis, nor in fibroblasts of the spiral ligament (Fig. 3B). In the spiral ganglion neurons and surrounding supporting cells in Rosenthal's canal, VDAC1/2/3 expression was similar to that of SLC2A1, as expression was only observed in the cytoplasm and nuclei of the neurons (Fig. 3C).

3.4. SLC22A1 (OCT1) transporter expression in the cochlear tissue

Immunohistochemical staining was also performed with antibodies to SLC22A1. In the organ of Corti, SLC22A1 protein was intensely expressed in the cytoplasm and nuclei of inner hair cells, and also in the cytoplasm of outer hair cells, but weakly expressed in surrounding support cells (Fig. 4A). SLC22A1 staining was also observed in the cytoplasm of three layers of stria vascularis, the marginal cells, intermediate cells, and basal cells (Fig. 4B). SLC22A1 was strongly expressed in the cytoplasm of spiral ganglion neurons, and weakly expressed in surrounding supporting cells (Fig. 4C).

Table 1
Normalized $2^{-\Delta CT}$ and average of three repeats of raw CT values. Values of highly expressed transporter genes in stria vascularis.

Symbol	Description	$2^{-\Delta CT}$	CT value
ATP6V0C	ATPase, H + transporting, lysosomal V0 subunit C	0.86	22.34
VDAC2	Voltage-dependent anion channel 2	0.75	22.53
VDAC1	Voltage-dependent anion channel 1	0.64	22.76
SLC3A2	Solute carrier family 3 (activators of dibasic and neutral amino ACID transport), member 2	0.56	22.96
SLC7A8	Solute carrier family 7 (cationic amino acid transporter, Y + system), member 8	0.33	23.73
SLC38A2	Solute carrier family 38, (sodium-dependent neutral amino acid transporter) member 2	0.21	24.35
SLC31A1	Solute carrier family 31 (high affinity copper transporter), member 1	0.15	24.81
SLC2A1	Solute carrier family 2 (facilitated glucose transporter), member 1	0.15	24.84

Table 2
Normalized $2^{-\Delta CT}$ and average of three repeats of raw CT values. Values of heavily expressed transporter genes in basilar membrane.

Symbol	Description	$2^{-\Delta CT}$	CT value
ATP6V0C	ATPase, H + transporting, lysosomal V0 subunit C	0.94	23.02
VDAC2	Voltage-dependent anion channel 2	0.76	23.34
VDAC1	Voltage-dependent anion channel 1	0.67	23.51
SLC3A2	Solute carrier family 3 (activators of dibasic and neutral amino acid transport), member 2	0.58	23.71
SLC7A8	Solute carrier family 7 (cationic amino acid transporter, Y + system), member 8	0.39	24.30
SLC38A2	Solute carrier family 38, (sodium-dependent neutral amino acid transporter) member 2	0.28	24.79
SLC3A1	Solute carrier family 3, (cystine and dibasic and neutral amino acid transporter) member 1	0.26	24.89

Table 3
Normalized $2^{-\Delta CT}$ and average of three repeats of raw CT values. Values of heavily expressed transporter genes in modiolus.

Symbol	Description	$2^{-\Delta CT}$	CT value
VDAC1	Voltage-dependent anion channel 1	1.19	22.31
ATP6V0C	ATPase, H + transporting, lysosomal V0 subunit C	0.98	22.59
VDAC2	Voltage-dependent anion channel 2	0.87	22.75
SLC3A1	Solute carrier family 3, (cystine and dibasic and neutral amino acid transporter) member 1	0.58	23.35
SLC22A2	Solute carrier family 22 (organic cation transporter), member 2	0.52	23.49
SLC38A2	Solute carrier family 38, (sodium-dependent neutral amino acid transporter) member 2	0.46	23.68
SLC3A2	Solute carrier family 3 (activators of dibasic and neutral amino acid transport), member 2	0.40	23.87
SLC7A8	Solute carrier family 7 (cationic amino acid transporter, y + system), member 8	0.19	24.93
ABCD3	ATP-binding cassette, subfamily D (ALD), member 3	0.19	24.96
SLC16A1	Solute carrier family 16, member 1 (monocarboxylic acid transporter 1)	0.17	25.10
SLC7A11	Solute carrier family 7 (cationic amino acid transporter, Y + system), member 11	0.16	25.16

3.5. SLC22A2 (OCT2) transporter expression in the cochlear tissue

The distribution of SLC22A2 was assessed and expression was found to be similar to that of SLC22A1 in the organ of Corti and stria vascularis (Fig. 5A and B). In the cochlear ganglion neurons, however SLC22A2 was only expressed in the cytoplasm and nuclei, while absent from surrounding support cells (Fig. 5C).

3.6. SLC3A2 (CD98) transporter expression in the cochlear tissue

The distribution of the neutral amino acid transporter, SLC3A2, was analyzed immunohistochemically and results reveal that it is expressed in the cytoplasm of both the cochlear hair cells and supporting cells (Fig. 6A). On the cochlear lateral wall, SLC3A2 was expressed in the cytoplasm of three layers of stria vascularis, the marginal cells, intermediate cells, and basal cells (Fig. 6B). In the cochlear ganglion neurons, SLC3A2 was specifically expressed in the nuclei of spiral ganglion neuron, but was not detected in surrounding support cells in the Rosenthal's canal (Fig. 6C).

3.7. SLC38A2 (SNAT2) transporter expression in the cochlear tissue

In the organ of Corti, SLC38A2 was expressed in the cytoplasm of cochlear outer hair cells, but weakly expressed in the inner hair and surrounding support cells (Fig. 7A). On the cochlear lateral wall, SLC38A2 was expressed in the cytoplasm of three layers of stria vascularis and capillaries (Fig. 7B). In the cochlear ganglion neurons, SLC38A2 was expressed in the cell membrane and nuclear envelope of spiral ganglion neuron, and also in the myelin sheath of auditory nerve fibers, but was not detected in surrounding support cells in the Rosenthal's canal (Fig. 7C).

4. Discussion

Accumulation of drugs within any given organ or cell in the body is dependent on the net uptake and export processes which are regulated by the differential expression and activity of the requisite transport proteins. Which of the two opposing transport processes actually limits the accumulation and overall effectiveness or deleterious actions of any drug is often cell specific as the levels and distribution of these transporters reside selectively within different cells of the body. This selectivity has been employed in the design of drugs to minimize side effects by preferentially targeting uptake into specific sites applicable for drug action. Enhanced cytotoxic outcomes can occur when exposures are greater than designed due to the inappropriate accumulation in non-targeted cells possessing the specific transport carriers.

The auditory system, being comprised of a distinct array of functioning elements, is particularly susceptible to the discriminating deposition of drugs that can potentially lead to hearing impairment. Several different classes of drugs have been reported to induce hearing deficits caused by the differential loss of distinct

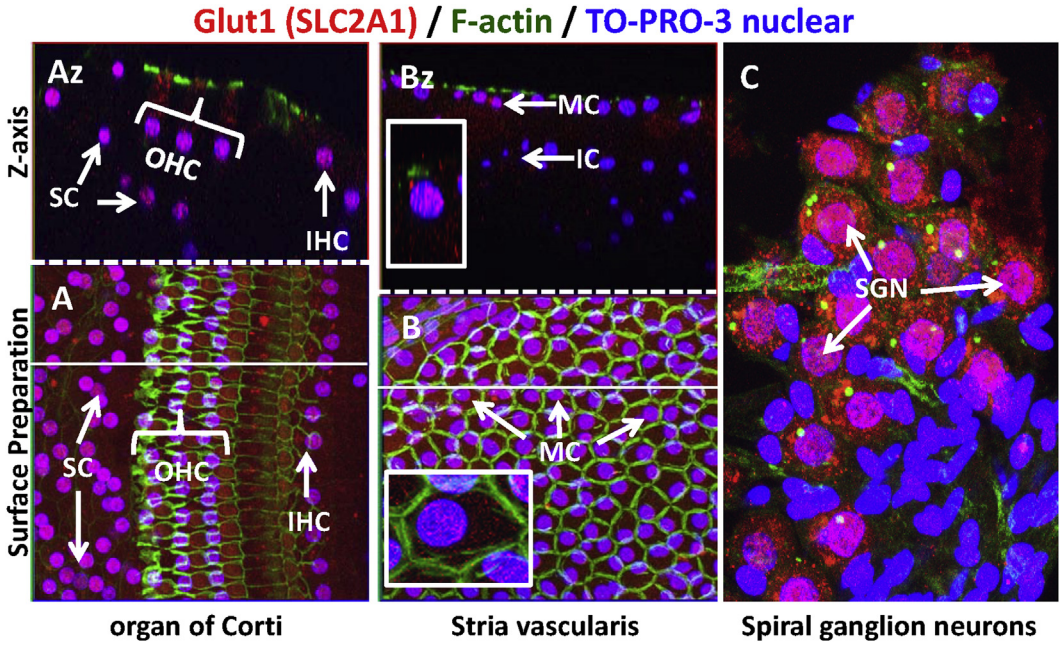

Fig. 2. Immunolocalization of Glut1 (SLC2A1) (red), F-actin (green) and TO-PRO-3 (blue) in cochlear tissue; pink reflects overlap of red and blue fluorescence. (A) Surface preparation view of organ of Corti showing Glut1 (pink) in nuclei of IHC, OHC and supporting cells (SC). (Az) Z-axis image of organ of Corti taken in the plane of the solid white line in A; note Glut1 in nuclei of OHC, IHC and SC. (B) Surface preparation of stria vascularis showing Glut1 (pink) in nuclei of marginal cells (MC) surrounded by green F-actin border. Inset shows higher magnification view of Glut1 labeling in marginal cell nucleus (pink). (Bz) Z-axis image of stria vascularis taken through the plane of the solid white line in B; note Glut1 (pink) in nuclei of MC. Inset shows higher magnification view of Glut1 labeling (pink) of marginal cell nucleus. Glut1 was absent from intermediate and deeper layers of stria vascularis. (C) Strong Glut1 labeling (pink) in nuclei of SGN in the modiolus. (For interpretation of the references to colour in this figure legend, the reader is referred to the web version of this article.)

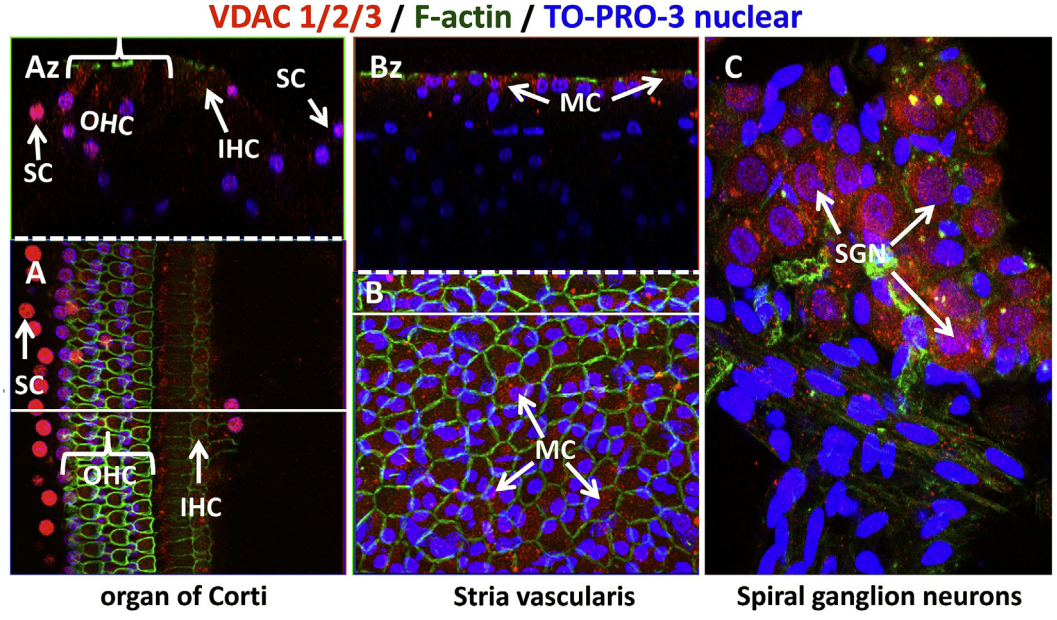

Fig. 3. Immunolocalization of VDAC 1/2/3 (red), F-actin (green) and TO-PRO-3 (blue) in cochlear tissue; pink reflects overlap of red and blue fluorescence. (A) Surface preparation view of organ of Corti showing VDAC 1/2/3 (red/pink) in nuclei and cytoplasm of IHC, OHC and supporting cells (SC). (Az) Z-axis image of organ of Corti taken in the plane of the solid white line in A; note VDAC 1/2/3 in nuclei of OHC, IHC and SC. (B) Surface preparation of stria vascularis showing VDAC 1/2/3 (red/pink) in marginal cells (MC) surrounded by green F-actin border. (Bz) Z-axis image of stria vascularis taken through the plane of the solid white line in B; note VDAC 1/2/3 (red/pink) in cytoplasm of MC. VDAC 1/2/3 largely absent from intermediate and deep layers of stria vascularis. (C) Strong VDAC 1/2/3 labeling (red/pink) in cytoplasm and nuclei of SGN in the modiolus. (For interpretation of the references to colour in this figure legend, the reader is referred to the web version of this article.)

cell populations within the inner ear. Ototoxic drugs include: nonsteroidal anti-inflammatory drugs (Davison and Marion, 1998) such as aspirin and ibuprofen, antibiotics, especially aminoglycosides (Brummett and Fox, 1989; Brummett and Morrison, 1990), loop diuretics that are used in the treatment of high blood pressure and heart failure, such as furosemide (Adelman et al., 2011; Pienkowski and Ulfendahl, 2011; Rais-Bahrami et al., 2004) and drugs to treat cancer which include cisplatin, carboplatin (Ding

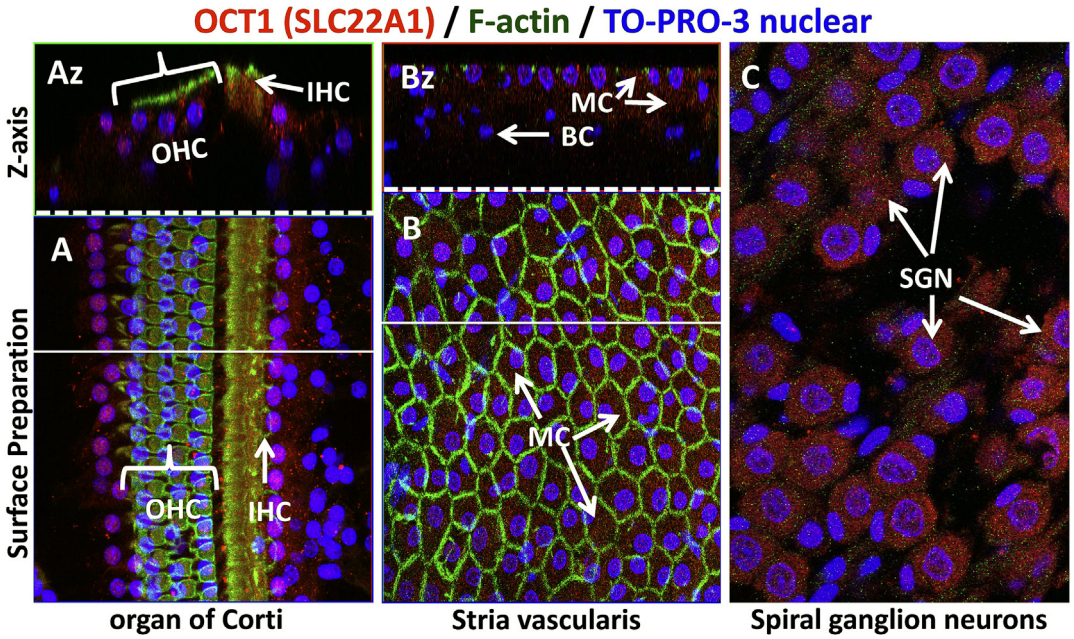

Fig. 4. Immunolocalization of OCT1 (SLC22A1) (red), F-actin (green) and TO-PRO-3 (blue) in cochlear tissue; pink reflects overlap of red and blue fluorescence. (A) Surface preparation view of organ of Corti showing OCT1 (pink) in nuclei and/or cytoplasm of IHC, OHC. (Az) Z-axis image of organ of Corti taken in the plane of the solid white line in A; note OCT1 in nuclei and/or cytoplasm mainly in OHC and IHC. (B) Surface preparation of stria vascularis showing OCT1 (pink) in marginal cell (MC) surrounded by green F-actin border. (Bz) Z-axis image of stria vascularis taken through the plane of the solid white line in B; note OCT1 (pink) in cytoplasm and nuclei of MC. OCT1 largely absent from intermediate and deep layers of stria vascularis. (C) Strong VDAC 1/2/3 labeling (red/pink) in cytoplasm and nuclei of SGN in the modiolus. (For interpretation of the references to colour in this figure legend, the reader is referred to the web version of this article.)

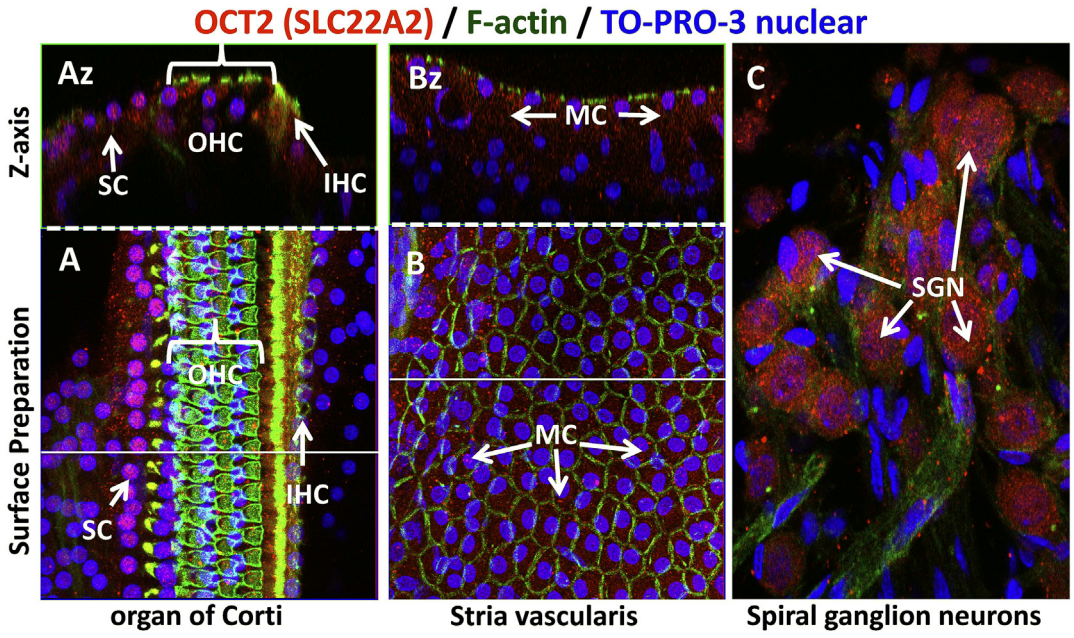

Fig. 5. Immunolocalization of OCT2 (SLC22A2) (red), F-actin (green) and TO-PRO-3 (blue) in cochlear tissue; pink reflects overlap of red and blue fluorescence. (A) Surface preparation view of organ of Corti showing OCT2 (red/pink) in nuclei and cytoplasm of IHC, OHC and SC. (Az) Z-axis image of organ of Corti taken in the plane of the solid white line in A; note OCT2 in nuclei of OHC, IHC and SC. (B) Surface preparation of stria vascularis showing OCT2 (red/pink) in marginal cells (MC) surrounded by green F-actin border. (Bz) Z-axis image of stria vascularis taken through the plane of the solid white line in B; note OCT2 (red/pink) in cytoplasm of MC. (C) Strong OCT2 labeling (red/pink) in cytoplasm and nuclei of SGN in the modiolus. (For interpretation of the references to colour in this figure legend, the reader is referred to the web version of this article.)

et al., 2012) and paclitaxel (Dong et al., 2014; Salvinelli et al., 2003). The extent and the nature of the injury as well as the hearing deficit produced by these drugs can vary and is dependent on the levels of the selective accumulaton of drugs within each of the different cellular components of the inner ear as well as possible differences in the mechanisms by which they induce cell death. Although not clearly quantified, transport into the cochlea and the subsequent selective uptake into the specialized elements is likely to be the rate-limiting step establishing the consequential outcomes of these ototoxins.

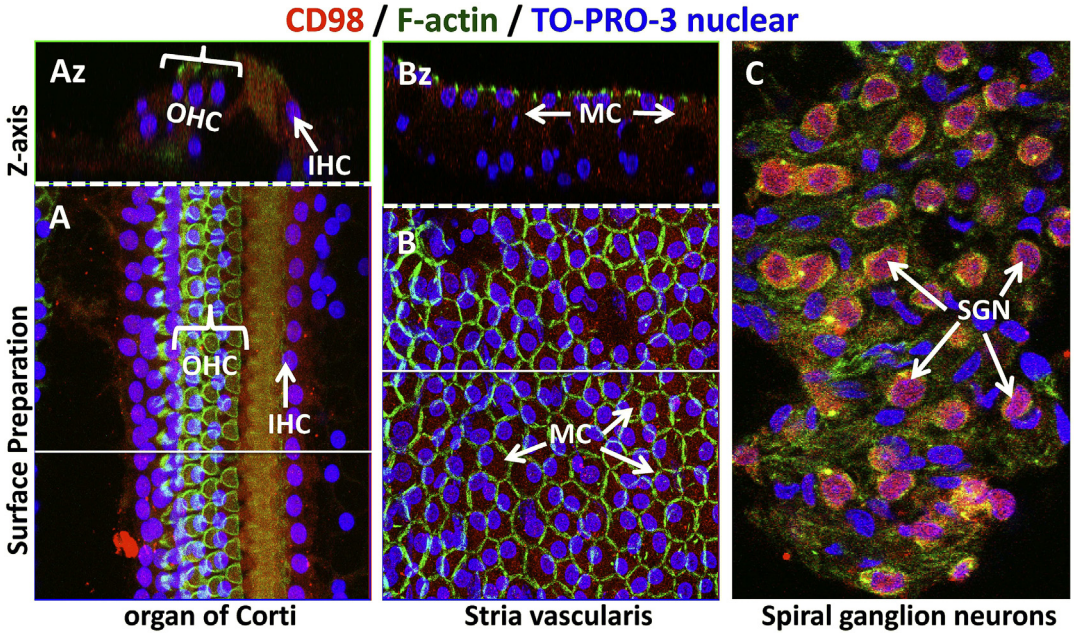

Fig. 6. Immunolocalization of CD98 (red), F-actin (green) and TO-PRO-3 (blue) in cochlear tissue; pink reflects overlap of red and blue fluorescence. (A) Surface preparation of organ of Corti showing CD98 (pink) in nuclei of IHC, OHC and SC. (Az) Z-axis image of organ of Corti taken in the plane of the solid white line in A; note CD98 in nuclei of OHC, IHC and SC. (B) Surface preparation of stria vascularis showing CD98 (pink) in marginal cells (MC) surrounded by green F-actin border. (Bz) Z-axis image of stria vascularis taken through the plane of the solid white line in B; note CD98 (pink) in cytoplasm of MC. (C) Strong CD98 labeling (red/pink) in nuclei of SGN in the modiolus. (For interpretation of the references to colour in this figure legend, the reader is referred to the web version of this article.)

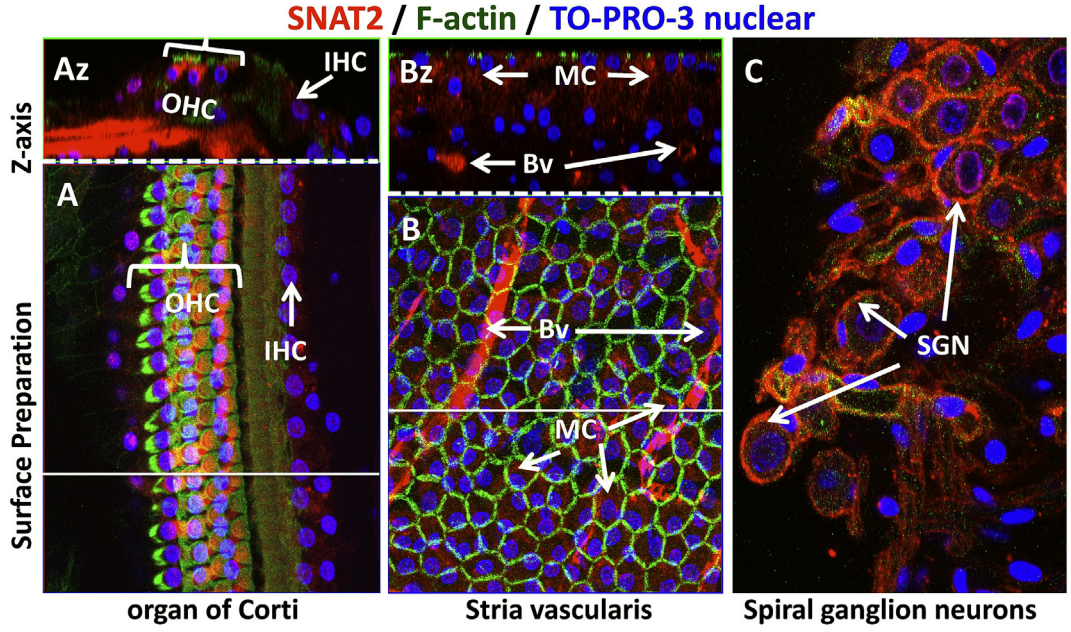

Fig. 7. Immunolocalization of SNAT2 (red), F-actin (green) and TO-PRO-3 (blue) in cochlear tissue; pink reflects overlap of red and blue fluorescence. (A) Surface preparation view of organ of Corti showing SNAT2 (red/pink) in cytoplasm and nuclei of IHC and OHC. (Az) Z-axis image of organ of Corti taken in the plane of the solid white line in A; note SNAT2 in cytoplasm and nuclei of OHC, IHC and SC. (B) Surface preparation of stria vascularis showing OCT2 (red/pink) in marginal cells (MC) surrounded by green F-actin border. (Bz) Z-axis image of stria vascularis taken through the plane of the solid white line in B; note OCT2 (red/pink) in cytoplasm of MC. (C) Strong OCT2 labeling (red/pink) in cytoplasm and nuclei of SGN in the modiolus. (For interpretation of the references to colour in this figure legend, the reader is referred to the web version of this article.)

In this paper we examined the expression of 84 different transporter genes in three different areas of the inner ear-the stria vascularis, the basilar membrane and the modiolus (Donaldson, 1975). The proteins encoded by these transporter genes likely play critical roles in the maintenance and function of the diverse cellular elements within the cochlea. The spiral ganglion neurons, located within the modiolus, are myelinated at their distal end by Schwann cells (Tuncel et al., 2005). The basilar membrane, which contains the sensory hair cells that transduce sound vibrations into neural activity are surrounded by a diverse array of supporting cells that not only provide structural support, but likely play a role in fluid transport, potassium recycling and maintenance of the

endolymphatic potential (Liu et al., 2015). The stria vascularis, which is highly vascularized, and the spiral ligament form the lateral wall of scala media. The marginal, intermediate and basal cells of the stria vascularis, in combination with the rich vascular bed, plays an important role in fluid and ion transport into scala media and the production of endolymph and +80 mV endolymphatic potential (Patuzzi, 2011).

A summary of the most highly expressed genes in the three areas of the inner ear is presented in Table 4. The most highly expressed genes in all three regions of the cochlea examined include ATP6V0C, VDAC1, VDAC2, SLC7A8, SLC3A2 and SLC38A2. In contrast, SLC3A1 was selectively expressed only in the modiolus and basilar membrane. SLC31A1 and SLC2A1 were highest in the stria vascularis whereas SLC16A1, SLC7A11, ABCD3 and SLC22A2 were most abundant within the basilar membrane. To a large extent, the majority of these are genes that encode proteins required for the normal maintenance of cellular function and include many of the amino acid and cation and anion transporters. Interestingly, the high affinity copper transporter protein, SLC31A1, shown to be responsible for the uptake of the anticancer, ototoxic drug cisplatin (Ciarimboli, 2014; Ding et al., 2011b), is most prominently expressed in the stria vascularis. The relatively high expression of this transporter in the stria vascularis suggests it may be, at least in part, a contributing factor influencing the ototoxic mechanism of cisplatin (Ding et al., 2012). Interestingly, both Oct1 and Oct2 have been associated with cisplatin uptake in kidney (Franke et al., 2010), although the role for these transporters in the inner ear have yet to be characterized. In contrast, the glucose transporter Glut1 (SLC2A1) that was detected prominently in hair cells and spiral ganglion neurons could provide protection against cisplatin ototoxicity, as Glut1 downregulation has been associated with cisplatin chemosensitivity (Wang et al., 2013).

The relative abundance of the genes examined in this study provides a fundamental and potentially useful compendium of proteins that may be critically important for the normal function of cells in the stria vascularis, basilar membrane and spiral ganglion. Mutations or post-translational modifications in one or more of these gene or protein transporters could contribute to unique forms of hearing loss and susceptibility to ototraumatic agents. Although some gene transporters were expressed at low levels, they may nevertheless contribute significantly to the transport of endogenous and exogenous molecules into specific cell types (i.e., inner hair cells), particularly during periods of stress induced by noise exposure or ototoxic drugs. The unique contribution each of these transporters plays in the function of specific cells within the cochlea is largely unknown, but is clearly of fundamental importance. Insights into their functional importance could be gleaned from genetic mutants, targeted deletions or specific pharmacologic manipulations. Moreover, the relative abundance of many of these transporter genes and the proteins which they encode are likely to be significantly up or down regulated by noise-exposure, genetic mutations, aging or exposure to ototoxic drugs. Identifying which transporters are up or downregulated, which cell types are affected and when these changes occur could provide novel insights on cochlear function and possible therapeutic interventions.

Table 4
Distribution of highly expressed transporters.

Stria vascularis	Basilar membrane	Modiolus
ATP6V0C	ATP6V0C	ATP6V0C
VDAC2	VDAC2	VDAC2
VDAC1	VDAC1	VDAC1
SLC7A8	SLC7A8	SLC7A8
SLC3A2	SLC3A2	SLC3A2
SLC38A2	SLC38A2	SLC38A2
–	SLC3A1	SLC3A1
SLC31A1	–	–
SLC2A1	–	–
–	–	SLC16A1
–	–	SLC7A11
–	–	ABCD3
–	–	SLC22A2

Conflicts of interest

The authors declare that there is no conflict of interests regarding the publication of this article.

Acknowledgments

This research was supported in part by grants from the National Institute for Occupational Safety and Health, R01 OH010235 and the National Institutes of Health, NIDCD 5R01DC011808.

References

Adelman, C., Weinberger, J.M., Kriksunov, L., Sohmer, H., 2011. Effects of furosemide on the hearing loss induced by impulse noise. J. Occup. Med. Toxicol. 6, 14.
Brummett, R.E., Fox, K.E., 1989. Aminoglycoside-induced hearing loss in humans. Antimicrob. Agents Chemother. 33, 797–800.
Brummett, R.E., Morrison, R.B., 1990. The incidence of aminoglycoside antibiotic-induced hearing loss. Arch. Otolaryngol. Head Neck Surg. 116, 406–410.
Camacho, J.A., Rioseco-Camacho, N., Andrade, D., Porter, J., Kong, J., 2003. Cloning and characterization of human ORNT2: a second mitochondrial ornithine transporter that can rescue a defective ORNT1 in patients with the hyperornithinemia-hyperammonemia-homocitrullinuria syndrome, a urea cycle disorder. Mol. Genet. Metab. 79, 257–271.
Ciarimboli, G., 2014. Membrane transporters as mediators of cisplatin side-effects. Anticancer Res. 34, 547–550.
Davison, S.P., Marion, M.S., 1998. Sensorineural hearing loss caused by NSAID-induced aseptic meningitis. Ear Nose Throat J. 77, 820-1–824-6.
De Mattia, E., Toffoli, G., Polesel, J., D'Andrea, M., Corona, G., Zagonel, V., Buonadonna, A., Dreussi, E., Cecchin, E., 2013. Pharmacogenetics of ABC and SLC transporters in metastatic colorectal cancer patients receiving first-line FOLFIRI treatment. Pharmacogenet. Genom. 23, 549–557.
Ding, D., Roth, J., Salvi, R., 2011a. Manganese is toxic to spiral ganglion neurons and hair cells in vitro. Neurotoxicology 32, 233–241.
Ding, D., Allman, B.L., Salvi, R., 2012. Review: ototoxic characteristics of platinum antitumor drugs. Anat. Rec. Hob. 295, 1851–1867.
Ding, D., He, J., Allman, B.L., Yu, D., Jiang, H., Seigel, G.M., Salvi, R.J., 2011b. Cisplatin ototoxicity in rat cochlear organotypic cultures. Hear. Res. 282, 196–203.
Donaldson, J.A., 1975. Normal anatomy of the inner ear. Otolaryngol. Clin. N. Am. 8, 267–269.
Dong, Y., Ding, D., Jiang, H., Shi, J.R., Salvi, R., Roth, J.A., 2014. Ototoxicity of paclitaxel in rat cochlear organotypic cultures. Toxicol. Appl. Pharmacol. 280, 526–533.
Drake, K.A., Torgerson, D.G., Gignoux, C.R., Galanter, J.M., Roth, L.A., Huntsman, S., Eng, C., Oh, S.S., Yee, S.W., Lin, L., Bustamante, C.D., Moreno-Estrada, A., Sandoval, K., Davis, A., Borrell, L.N., Farber, H.J., Kumar, R., Avila, P.C., Brigino-Buenaventura, E., Chapela, R., Ford, J.G., Lenoir, M.A., Lurmann, F., Meade, K., Serebrisky, D., Thyne, S., Rodriguez-Cintron, W., Sen, S., Rodriguez-Santana, J.R., Hernandez, R.D., Giacomini, K.M., Burchard, E.G., 2014. A genome-wide association study of bronchodilator response in Latinos implicates rare variants. J. Allergy Clin. Immunol. 133, 370–378.
Franke, R.M., Kosloske, A.M., Lancaster, C.S., Filipski, K.K., Hu, C., Zolk, O., Mathijssen, R.H., Sparreboom, A., 2010. Influence of Oct1/Oct2-deficiency on cisplatin-induced changes in urinary N-acetyl-beta-D-glucosaminidase. Clin. Cancer Res. 16, 4198–4206.
Greenberg, R.M., 2013. ABC multidrug transporters in schistosomes and other parasitic flatworms. Parasitol. Int. 62, 647–653.
Hawley, T.S., Riz, I., Yang, W., Wakabayashi, Y., Depalma, L., Chang, Y.T., Peng, W., Zhu, J., Hawley, R.G., 2013. Identification of an ABCB1 (P-glycoprotein)-positive carfilzomib-resistant myeloma subpopulation by the pluripotent stem cell fluorescent dye CDy1. Am. J. Hematol. 88, 265–272.
Ishikawa, T., Sakurai, A., Kanamori, Y., Nagakura, M., Hirano, H., Takarada, Y., Yamada, K., Fukushima, K., Kitajima, M., 2005. High-speed screening of human ATP-binding cassette transporter function and genetic polymorphisms: new strategies in pharmacogenomics. Methods Enzymol. 400, 485–510.
Kobayashi, K., Ohzono, H., Shinohara, M., Saitoh, M., Ohmori, I., Ohtsuka, Y., Mizuguchi, M., 2012. Acute encephalopathy with a novel point mutation in the SCN2A gene. Epilepsy Res. 102, 109–112.
Letschert, K., Keppler, D., Konig, J., 2004. Mutations in the SLCO1B3 gene affecting the substrate specificity of the hepatocellular uptake transporter OATP1B3

(OATP8). Pharmacogenetics 14, 441–452.
Liu, W., Atturo, F., Aldaya, R., Santi, P., Cureoglu, S., Obwegeser, S., Glueckert, R., Pfaller, K., Schrott-Fischer, A., Rask-Andersen, H., 2015. Macromolecular organization and fine structure of the human basilar membrane – relevance for cochlear implantation. Cell Tissue Res. 360, 245–262.
Patuzzi, R., 2011. Ion flow in stria vascularis and the production and regulation of cochlear endolymph and the endolymphatic potential. Hear. Res. 277, 4–19.
Pienkowski, M., Ulfendahl, M., 2011. Differential effects of salicylate, quinine, and furosemide on Guinea pig inner and outer hair cell function revealed by the input-output relation of the auditory brainstem response. J. Am. Acad. Audiol. 22, 104–112.
Rais-Bahrami, K., Majd, M., Veszelovszky, E., Short, B.L., 2004. Use of furosemide and hearing loss in neonatal intensive care survivors. Am. J. Perinatol. 21, 329–332.
Roth, M., Obaidat, A., Hagenbuch, B., 2012. OATPs, OATs and OCTs: the organic anion and cation transporters of the SLCO and SLC22A gene superfamilies. Br. J. Pharmacol. 165, 1260–1287.
Salvinelli, F., Casale, M., Vincenzi, B., Santini, D., Di Peco, V., Firrisi, L., Onori, N., Greco, F., Tonini, G., 2003. Bilateral irreversible hearing loss associated with the combination of carboplatin and paclitaxel chemotherapy: a unusual side effect. J. Exp. Clin. Cancer Res. 22, 155–158.
Seow, H.F., Broer, S., Broer, A., Bailey, C.G., Potter, S.J., Cavanaugh, J.A., Rasko, J.E., 2004. Hartnup disorder is caused by mutations in the gene encoding the neutral amino acid transporter SLC6A19. Nat. Genet. 36, 1003–1007.
Thompson, B.J., Jessen, T., Henry, L.K., Field, J.R., Gamble, K.L., Gresch, P.J., Carneiro, A.M., Horton, R.E., Chisnell, P.J., Belova, Y., McMahon, D.G., Daws, L.C., Blakely, R.D., 2011. Transgenic elimination of high-affinity antidepressant and cocaine sensitivity in the presynaptic serotonin transporter. Proc. Natl. Acad. Sci. U. S. A. 108, 3785–3790.
Torres, A.M., Dnyanmote, A.V., Bush, K.T., Wu, W., Nigam, S.K., 2011. Deletion of multispecific organic anion transporter Oat1/Slc22a6 protects against mercury-induced kidney injury. J. Biol. Chem. 286, 26391–26395.
Tuncel, M., Surucu, H.S., Erbil, K.M., Konan, A., 2005. Formation of the cochlear nerve in the modiolus of the guinea pig and human cochleae. Arch. Med. Res. 36, 436–440.
Wang, Y.D., Li, S.J., Liao, J.X., 2013. Inhibition of glucose transporter 1 (GLUT1) chemosensitized head and neck cancer cells to cisplatin. Technol. Cancer Res. Treat. 12, 525–535.
Wen, P.C., Verhalen, B., Wilkens, S., McHaourab, H.S., Tajkhorshid, E., 2013. On the origin of large flexibility of P-glycoprotein in the inward-facing state. J. Biol. Chem. 288, 19211–19220.